Spiroconjugation in Spirodicorrolato-Dinickel(II)

Georg Hohlneicher,*[a] Dominik Bremm,[a] Jennifer Wytko,[b] Jordi Bley-Escrich,[b] Jean-Paul Gisselbrecht,[b] Maurice Gross,[b] Martin Michels,[c] Johann Lex,[c] and Emanuel Vogel[c]

Dedicated to Professor Jack Dunitz on the occasion of his 80th birthday

Abstract: In the present work the effect of spiroconjugation on the electronic spectrum of the recently synthesized metal complex hexadecaethylspirodicorrolato–dinickel(II) (**5**) (the corrole units in **5** are isoforms) is investigated. To have a suitable reference compound at our disposal, tetraethylhexamethylisocorrolato nickel(II) (**7**) has been prepared. On comparing the electronic spectra of this reference compound and the spiro-complex, bathochromic shifts of all absorption bands in the NIR/Vis-region are observed for the latter as well as marked changes in the spectral intensities. A detailed analysis of the spectra supported by semiempirical calculations reveals that at least part of the observed changes can be unambiguously attributed to the spiro effect. This effect is further affirmed by electrochemically measured redox potentials.

Keywords: electrochemistry · electron spectroscopy · porphyrinoids · spiro compounds · spiroconjugation

Introduction

On exploration of the chemistry of *Figure Eight* cyclooctapyrroles[1] our attention was drawn to spirodicorrole (**1**), a representative of the as yet unknown class of spirodiporphyrinoids. Structurally, **1** consists of two corrole units linked through a spiro center and thus held in an orthogonal position. As a consequence of this linkage, the corrole units adopt the character of isoforms,[2] in which the number of inner NH protons is reduced to two compared with three in corrole. Accordingly, **1** should be particularly well suited to form complexes with divalent metals. A case in point is the nickel complex **2.**[3]

Spirodicorrole (**1**) and its metal complexes, such as **2**, command theoretical interest with regard to chemical bonding since they are candidates for the occurrence of spiroconjugation, a concept first postulated by Simmons and Fukunaga[4] as well as by Hoffmann, Imamura and Zeiss.[5,6]

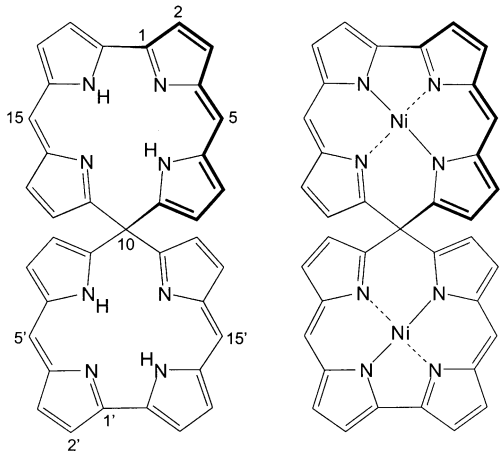

1 **2**

As illustrated in Figure 1, spiroconjugation constitutes a special kind of homoconjugative interaction that depends on the presence of two π-electron systems arranged in perpendicular planes by a common spiro carbon atom, as is the case in **1** and **2**. The overlap integral of the orbitals in the two planes is estimated to reach approximately 10% of the value for adjacent p-orbitals in planar π-systems.[5] Bearing in mind that spiro compounds exhibit a total of four orbital

[a] Prof. Dr. G. Hohlneicher, D. Bremm
Institut für Physikalische Chemie der Universität zu Köln
Luxemburger Strasse 116, 50939 Köln (Germany)
Fax: (+49) 221-470-5144
E-mail: gehohln@pc.uni-koeln.de

[b] Dr. J. Wytko, J. Bley-Escrich, Dr. J.-P. Gisselbrecht, Prof. Dr. M. Gross
Laboratoire d'Electrochimie et de Chimie Physique de Corps Solide
UMR 7512-CNRS, Université Louis Pasteur
4, rue Blaise Pascal, 67000 Strasbourg (France)

[c] Dr. M. Michels, Dr. J. Lex, Prof. Dr. E. Vogel
Institut für Organische Chemie der Universität zu Köln
Greinstrasse 4, 50939 Köln (Germany)

© 2003 Wiley-VCH Verlag GmbH & Co. KGaA, Weinheim
DOI: 10.1002/chem.200305094

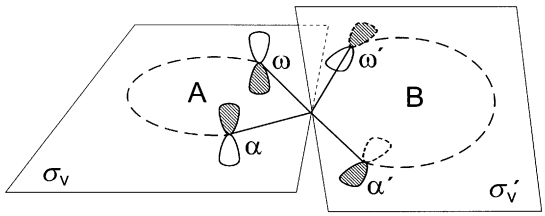

Figure 1. Orbital interaction in a spiro compound with orthogonal π systems.

interactions of the kind shown in Figure 1, spiroconjugation is bound to have a noticeable effect on the MO energy levels. From perturbation theory it is apparent that this effect should be most pronounced if the two spiro-bonded subunits are identical.[7] In fact, the occurrence of spiroconjugation has been demonstrated for a variety of molecules of this type by using either photoelectron[8] or electronic spectroscopy (UV/Vis).[9] In addition, the consequences of the effect on the reactivity and structure of spiro compounds have been discussed.[10]

To prove the occurrence of spiroconjugation spectroscopically, it is necessary to compare the photoelectron and/or electronic spectrum of the spiro compound in question with the spectrum of a suitable reference compound that represents the two separated π-electron systems. Clearly, in the case of **1**, the most appropriate reference would be 10,10-dimethylisocorrole (**3**), as shown below together with the corresponding nickel complex **4**.

While the parent spirodicorrole **1** and its metal complexes are still elusive, the nickel complex **5** of an alkyl derivative of **1**, that is, hexadecaethylspirodicorrolato–dinickel(II), has recently been discovered. Accordingly, we used

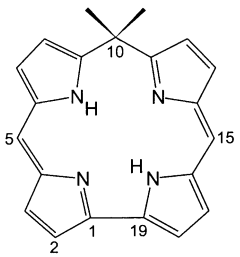

3

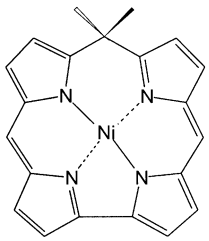

4

5 as a substrate to investigate spiroconjugation in spirodicorroles of this type. As the low vapour pressure of **5** rules out the application of photoelectron spectroscopy, we used electron spectroscopy in parallel with semiempirical calculations at the INDO/S-CIS level to interpret the experimental findings. The obvious reference for **5**, namely 2,3,7,8,12,13,17,18-octaethyl-10,10-dimethylisocorrolato–nickel(II) (**6**), unexpectedly defied synthesis. Thus the closely related 2,3,17,18-tetraethyl-7,8,10,10,12,13-hexamethylisocorrolato–nickel(II) (**7**), which could be prepared straightforwardly, served as the reference.

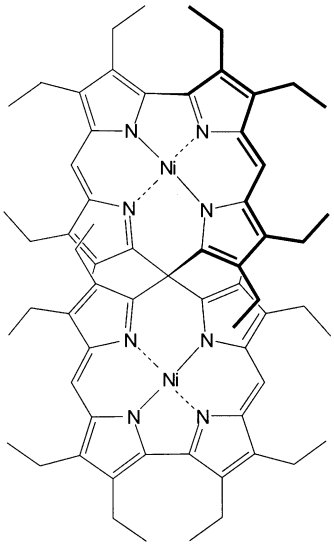

5

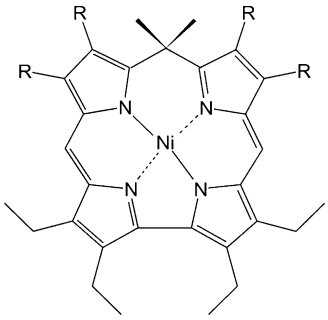

6: R = C_2H_5
7: R = CH_3

Results and Discussion

The key compound of the present investigation, the nickel complex **5** of hexadecaethylspirodicorrole, was not obtained by a planned synthesis, but resulted from an unexpected cascade of reactions occurring upon treatment of octaphyrin(1.1.1.0.1.1.1.0)[1] (as the hexadecaethyl derivative) with nickel(II)acetate in boiling DMF.[3] The structure of **5** follows, apart from the NMR spectra, from an X-ray crystallographic analysis that shows that the two metallocorrole subunits are oriented almost orthogonally. As inferred from the near planarity and rigidity of these subunits, the nickel ions must be bound very tightly. It is therefore hardly surprising that all efforts to bring about demetalation of **5** to give the free ligand have so far been futile.

The synthesis of **6**, the envisaged reference compound for **5**, depended on the availability of bis(2-benzyloxycarbonyl-3,4-diethylpyrryl)dimethylmethane (**9**) as a building block. However, the obvious way of generating **9**, by acid-catalyzed condensation of 2-benzyloxycarbonyl-3,4-diethylpyrrole[11] (**8**) with acetone failed, presumably because of steric hindrance (Scheme 1). As **10,** the methyl analogue of **9,** had previously been described by Smith et al.,[12] it seemed logical to resort to **7** as the reference compound for **5**.

Taking advantage of established procedures in corrole chemistry, conversion of **10** into the target molecule **7** was achieved as follows (see Scheme 2): The bis(benzylester) **10** was easily reduced by 10% palladium on activated carbon

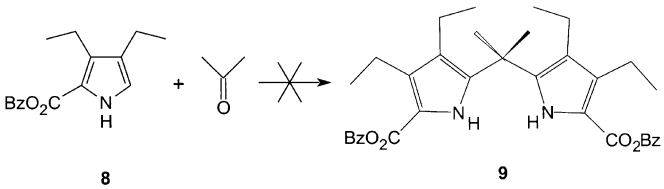

8 **9**

Scheme 1. Envisaged synthesis of bis(2-benzyloxycarbonyl-3,4-diethylpyrryl)dimethylmethane **9**.

 © 2003 Wiley-VCH Verlag GmbH & Co. KGaA, Weinheim

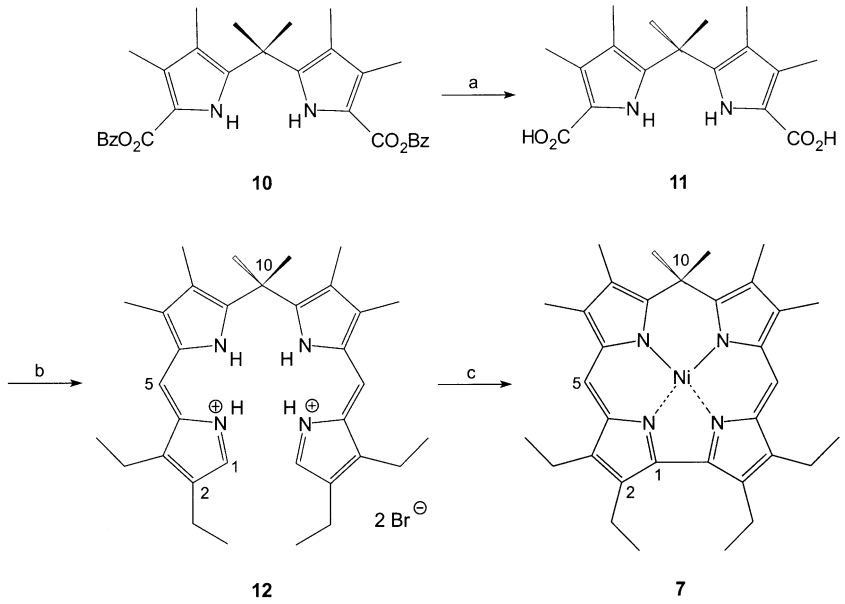

Scheme 2. Synthesis of 2,3,17,18-tetraethyl-7,8,10,10,12,13-hexamethylisocorrolato–nickel(II) **7**: a) 10% Pd/C, H_2, THF; b) 2 equiv 3,4-diethyl-2-formylpyrrole, 48% HBr (aq), EtOH, Δ; 56%; c) i) $Ni(OAc)_2 \cdot 4H_2O$; MeOH; ii) chloranil; 68%.

to give the diacid **11** which, without isolation, was condensed with 3,4-diethyl-2-formylpyrrole[11] in refluxing methanol in the presence of 48% aqueous hydrobromic acid. After conventional work-up, a greenish-black solid was isolated, which proved to be the biladiene-*ac*-dihydrobromide **12**. When salt **12** was treated with nickel acetate in methanol and then with chloranil, the desired nickel complex **7** started to precipitate as tiny crystals within minutes. Recrystallization of this material from chloroform/methanol yielded **7** as blue-violet needles. The structure of **7**, which is fully consistent with the ^1H and ^{13}C NMR spectra (see Experimental Section), was established unequivocally by X-ray analysis.[13] As expected, the skeleton of the complex is planar and exhibits C_{2v} symmetry (Figure 2). In addition, the structural data of **7** closely match those of the spirodicorrole nickel complex **5** , a fact that lends further support to its use as the reference compound.

Figure 3 shows the low energy part of the UV/Vis/NIR spectra of the complexes **5** and **7**. The spectra of both compounds consist of three band systems, one of medium intensity between 9000 cm^{-1} and 14000 cm^{-1} (labeled A in Figure 3) and two intense ones (labeled B and C) between 14000 cm^{-1} and 30000 cm^{-1}. The bands of the spiro compound display a bathochromic shift of 2000–2500 cm^{-1} and have considerably different spectral intensities with respect to the reference compound. The goal of this investigation is to find out whether these changes are indicative of spiroconjugation or not. Prior to this, however, the observed bands have to be assigned.

In the solid state, the methyl groups of the ethyl substituents of **5** and **7** are oriented more or less perpendicularly to the ring planes (see Figure 2 and ref. [3]). In solution, the flexible side chains will most likely attain a more random orientation; this makes it difficult to select a certain geometry for the calculations. For this reason, and considering the fact that alkyl side chains attached to the pyrrole rings of porphyrinoids generally have a relatively modest influence on the electronic spectra of these compounds, the assignment of the experimental spectra was based on INDO/S results for the unsubstituted complexes **2** and **4**. The equilibrium structures of these compounds were obtained by full geometry optimization at the DFT level. In both cases the calculations led to geometries of the highest possible symmetry—D_{2d} for **2** and C_{2v} for **4**. The calculated bond lengths and angles agree very well with those derived from the X-ray analysis for the skeletons of complexes **5** and **7**. To ensure that the neglect of the alkyl side chains does not lead to any misinterpretation, we also calculated the INDO/S spectra of **5** and **7** employing the available X-ray geometries. The differences between these spectra and those calculated for **2** and **4** turned out to be far too small to influence the assignment of bands and band shifts significantly.

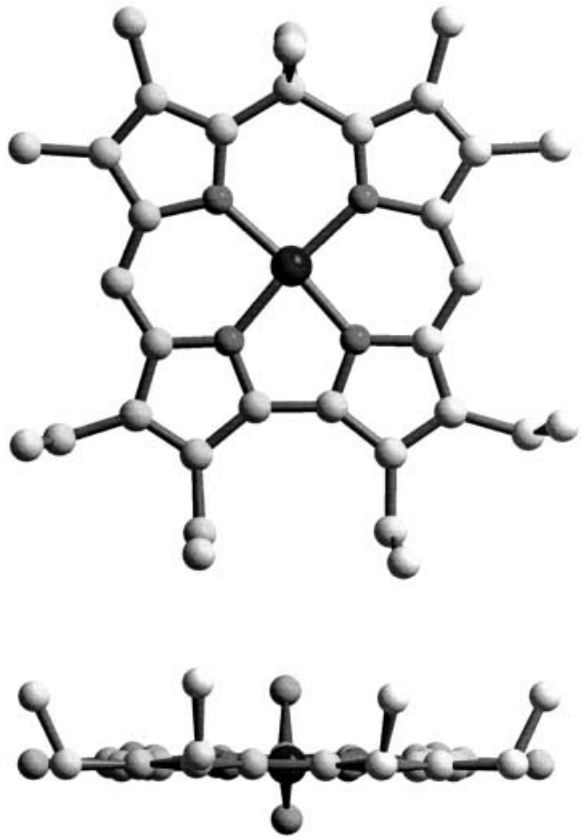

Figure 2. X-ray structure of **7**: top, front view; bottom, side view.

© 2003 Wiley-VCH Verlag GmbH & Co. KGaA, Weinheim

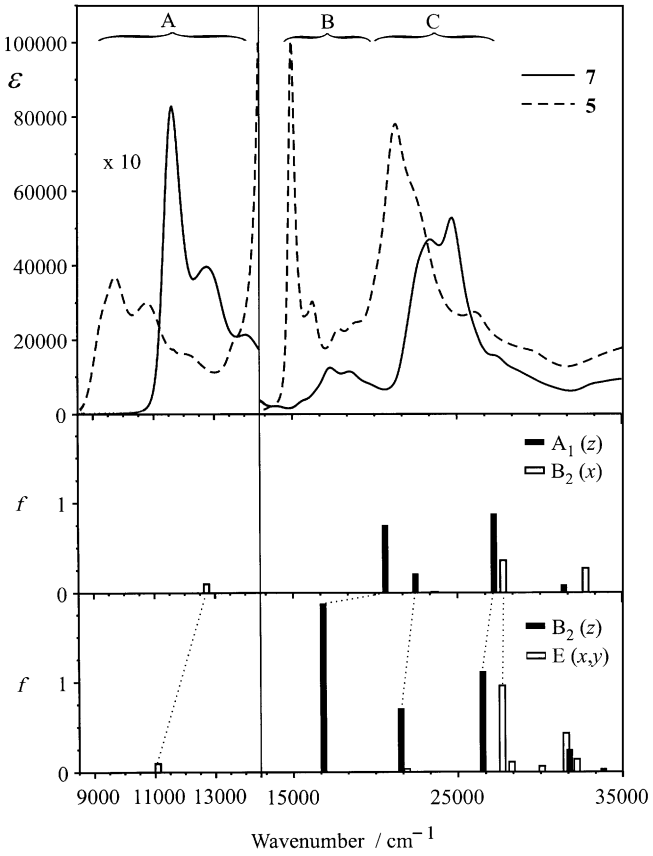

Figure 3. Top: experimental spectra of **7** and **5** in CH_2Cl_2 at 298 K. Center: INDO/S-spectrum of **4**. Bottom: INDO/S-spectrum of **2**.

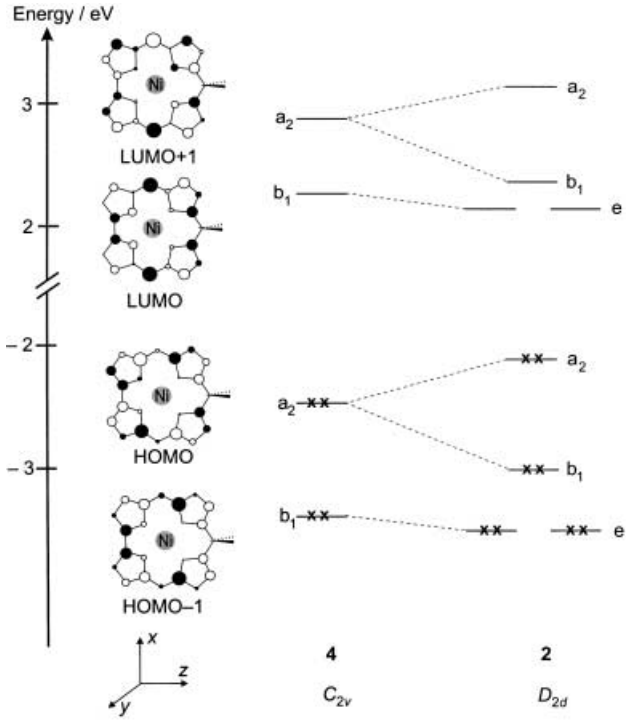

Figure 4. Correlation of the highest-occupied and the lowest-unoccupied orbitals of **4** and **2**.

Before proceeding, it is instructive to take a look at the orbital diagram that results from the INDO/S calculations (Figure 4). a_2 orbitals of **4** (point group C_{2v}) correlate with two orbitals of **2** (point group D_{2d}) that are energetically split. This splitting is a direct consequence of spiroconjugation. b_1 orbitals do not interact and correlate with a degenerate pair of orbitals in **2**. The calculations predict a split of 0.9 eV (7200 cm^{-1}) for the HOMO of **4** and a split of 0.8 eV (6400 cm^{-1}) for the LUMO+1. Ab initio Hartree–Fock calculations with a 6-31G* basis set yield similar results (0.8 eV for the HOMO and 1.1 eV for the LUMO+1) and confirm the occurrence of spiroconjugation at least on the purely theoretical level.

A first experimental hint as to the correctness of this result comes from the electrochemical data obtained in benzonitrile. Six reversible one-electron redox steps could be observed for **5**, two reductions at $E_{Red1} = -1.59$ V/Fc and $E_{Red2} = -1.97$ V/Fc, and four oxidations at $E_{Ox1} = -0.23$ V/Fc, $E_{Ox2} = +0.16$ V/Fc, $E_{Ox3} = +0.77$ V/Fc, and $E_{Ox4} = +0.86$ V/Fc. For **7**, only four reversible one-electron steps were observed, two reductions at $E_{Red1} = -1.72$ V/Fc and $E_{Red2} = -2.32$ V/Fc, and two oxidations at $E_{Ox1} = -0.14$ V/Fc and $E_{Ox2} = +0.37$ V/Fc. The difference between the first oxidation and the first reduction potential is reduced by 0.22 V on going from **7** (1.58 V) to **5** (1.36 V). This correlates with the predicted reduction of the HOMO/LUMO gap (0.47 eV semiempirical, 0.71 eV ab initio). The fact that the individual shifts (+0.13 V for the first reduction and −0.09 V for the first oxidation potential) agree only in their tendency (down for the LUMO and up for the HOMO) with the theoretical results is not surprising. The redox potentials of the two systems cannot be compared on an absolute scale because of possible differences in solvatation. However, at least in the solvent benzonitrile these unknown differences do not change the order predicted for the free molecules: the spiro compound is more easily oxidized than the reference compound. The fact that, in the experimentally accessible potential range, four oxidation steps were found for **5** but only two for **7** is also in agreement with the orbital picture shown in Figure 1. If the HOMO−1 in **7** is too low to be observed, the corresponding orbitals in **5** (HOMO−3 and HOMO−4) should also be too low. Nevertheless, the two orbitals that result from the splitting of the HOMO of the reference compound should be observable in the spiro compound. If the four oxidation steps in **5** are assigned to the removal of the four electrons in the HOMO and the HOMO−1, the difference between the average of the first two oxidation potentials and the average of the second two should yield a rough estimate of the splitting caused by spiroconjugation. The resulting value of 0.85 V compares reasonably well with the theoretical predictions mentioned above.

With the INDO/S results (Figure 2 and Table 1) in hand, the assignment of the spectra in regions A and B becomes an easy task. The bands in region A result from a medium-intensity transition, which in both cases is dominated by the HOMO→LUMO excitation. In **2** as well as in **4** the transitions are polarized perpendicular to the z-axis (see Figure 4 for the definition of the coordinate system). In **2** the transition is degenerate but the calculated intensity—expressed by the oscillator strength—is nearly the same as in **4**.[14] In

 © 2003 Wiley-VCH Verlag GmbH & Co. KGaA, Weinheim

Table 1. Calculated and experimental spectral parameters. Excitation energies are given in cm^{-1}. Oscillator strengths are quoted in parenthesis. The theoretical data refer to the unsubstituted compounds **4** and **2**, the experimental ones to **7** and **5**.

state	INDO/S-CIS	experiment	leading configuration
		reference compound	
$1\,^1B_2$	12720 (0.097)	11600 (0.041)	HOMO→LUMO
$2\,^1A_1$	20630 (0.752)	17320 (0.14)[a]	HOMO→LUMO+1
$3\,^1A_1$	22450 (0.212)		HOMO−1→LUMO
$4\,^1A_1$	27210 (0.877)	ca. 23950 (0.61)[b]	HOMO−2→LUMO
$4\,^1B_2$	27770 (0.354)		HOMO−1→LUMO
		spiro compound	
$1\,^1E$	11090 (0.095)	9740 (0.030)	HOMO→LUMO
$1\,^1B_2$	16820 (1.872)	14970 (0.31)[c]	HOMO→LUMO+1
$2\,^1B_2$	21550 (0.706)	17900?	HOMO−2→LUMO
$3\,^1B_2$	26500 (1.119)	ca. 21850 (0.85)[d]	HOMO−5→LUMO
$8\,^1E$	27690 (0.958)		HOMO−2→LUMO

Oscillator strengths: [a] 14800 to 20700 cm^{-1} region. [b] 20700 to 27000 cm^{-1} region. [c] 13200 to 19200 cm^{-1} region. [d] 19200 to 25100 cm^{-1} region.

the experimental spectra the intensity is slightly lower for the spiro compound than for the reference compound (the experimental oscillator strengths are included in Table 1). The calculated bathochromic shift is 1600 cm^{-1} as compared to an experimental value of 1900 cm^{-1}.

For region B the calculation predicts two *z*-polarized transitions for reference compound **4**, both of which are assigned to the band observed between 14800 cm^{-1} and 20700 cm^{-1} in the spectrum of **7**. The spectrum of **5** shows an indication of two separate bands in this region. Such a separation is in accordance with the INDO/S results, which predict a much stronger bathochromic shift for the first of the two *z*-polarized transitions (3800 cm^{-1}) than for the second one (900 cm^{-1}). The experimental shift between the two band maxima is 2300 cm^{-1}.

In region C, a bathochromic shift of 2000 cm^{-1} is again observed for the spiro compound but a detailed assignment of the corresponding bands is difficult. The calculations predict two transitions with opposite polarization which are too close to assure that the predicted order is correct. It is also questionable as to whether CI calculations that only include singly excited configurations are sufficient to describe these higher excited states. To reach a more definitive assignment it is necessary to determine the polarization experimentally. In the case of **7** this was attempted by measurements with polarized light on samples of the compound contained in a stretched polyethylene sheet, but no linear dichroism was detected.

At least for the first two band systems (A and B) the calculations reproduce the differences between the reference and the spiro compounds. But how indicative are these differences for the occurrence of spiroconjugation? When trying to answer this question it must be taken into account that changes in spectroscopic parameters between spiro and reference compounds are not only due to this special kind of homoconjugative interaction. Other possible causes of such changes are field effects between the two moieties, inductive effects at the spiro center,[9e] and, last but not least, exciton coupling between the two partial chromophores.[15] To check for a possible inductive effect we calculated the spectrum of the hypothetical 10,10-difluoroisocorrole. Even with fluorine atoms as highly electronegative substituents, the largest shift relative to **4** was only 900 cm^{-1} for all transitions below 30000 cm^{-1}, and the calculated intensities showed little change. It is therefore very unlikely that an inductive effect is the reason for the observed differences. Field effects should play a minor role in the present case because of the fairly uniform charge distribution in the two moieties. We are therefore left with exciton coupling as the main competitor to spiroconjugation.

In molecules with D_{2d} symmetry, exciton coupling leads to an interaction between transitions that are *z*-polarized in the partial chromophores (symmetry A_1). In a first-order approximation, the exciton coupling splits each *z*-polarized transition into two, the lower component of which obtains a doubled intensity relative to the partial chromophore, while the higher component is forbidden. The magnitude of the interaction and therefore of the split increases with the intensity of the transition. Transitions that are polarized perpendicular to *z* in the partial chromophores (symmetry B_2) do not interact. They remain degenerate in the spiro compound and their intensity should be twice as high as in the partial chromophore.

As the first transition in **4** is polarized perpendicular to *z*, there is no exciton coupling for this transition in **2**. If exciton coupling were the dominating effect, a doubling of the intensity and practically no shift should be found. Comparison of **5** with **7** actually shows a bathochromic shift of almost 2000 cm^{-1} and a slightly reduced intensity. Thus, these changes cannot be caused by exciton coupling. However, the observed shift is easily understood when one takes into consideration that spiroconjugation raises the energy of the HOMO and leaves the LUMO unchanged.

In region B of the spectrum, the situation is more complicated. The two transitions that can be assigned to the band appearing in this region in the spectrum of **7** are *z*-polarized. In the spiro compound they are influenced by spiroconjugation as well as by exciton coupling and it is not a priori clear whether or not the observed shift provides further information on spiroconjugation. We therefore tried to estimate the magnitude of the exciton coupling.[15] A calculation based on the dipole approximation with the experimental oscillator strength of the second band of **7** (Table 1) together with the known geometric parameters yields an exciton splitting energy of only 550 cm^{-1}. This is certainly an upper limit because the intensity of the second band of **7** results from two different transitions. This split is much too small to explain the experimentally observed shift of more than 2000 cm^{-1}. When one takes spiroconjugation into account the shift is again easily understood: the second transition in **4** as well as in **2** results mainly from an excitation from the HOMO into the LUMO+1. Spiroconjugation

© 2003 Wiley-VCH Verlag GmbH & Co. KGaA, Weinheim

lowers the energy of the LUMO+1 and raises the energy of the HOMO (Figure 4), both of which lead to a reduction in the energy for the HOMO→LUMO+1 excitation. On a qualitative level this even explains the larger shift in the second transition compared with the first: for the first transition only the lower energy level (HOMO) is affected by spiroconjugation. The fact that the increase in intensity in region B exceeds a factor of two in the experiment as well as in the calculation provides additional evidence for the occurrence of spiroconjugation in the spiro compounds **2** and **5**.

Conclusion

With the synthesis of tetraethylhexamethylisocorrolato–nickel(II) (**7**) we obtained a suitable reference compound for hexadecaethylspirodicorrolato–dinickel(II) (**5**) that allowed us to study the occurrence of spiroconjugation in spirodicorroles. Investigation of the electronic spectra in connection with theoretical calculations leaves little doubt that spirodicorroles are indeed systems in which spiroconjugation is of considerable importance for a variety of molecular properties. These findings are corroborated by electrochemically determined oxidation potentials, which show that **5** is more easily oxidized because of the influence of spiroconjugation on the HOMO. The influence of the reduced oxidation potential on the reactivity of spirodicorroles will be the subject of further studies.

Experimental Section

Synthesis of 2,3,17,18-Tetraethyl-7,8,10,10,12,13-hexamethylisocorrolato nickel(II) (7)

*7,8,10,10,12,13-Hexamethyl-2,3,17,18-tetraethylbiladiene-ac-dihydrobromide (**12**)*: A mixture of bis-(2-benzyloxycarbonyl-3,4-dimethylpyrryl)dimethylmethane **10** (249 mg, 0.5 mmol) and 10% palladium on activated carbon (200 mg) in dry THF (30 mL) containing triethylamine (0.5 mL) was degassed with hydrogen, then vigorously stirred under a hydrogen atmosphere. After 45 min, the mixture was filtered, and the solvent was removed in vacuo. The residual diacid **11** was dissolved in warm EtOH (10 mL) and THF (0.5 mL), then 3,4-diethyl-2-formylpyrrole (166 mg, 1.1 mmol) was added. The solution was heated to 60°C then HBr (aq) (48%, 1.5 mL) was added. The resulting deep red solution was heated under reflux for 5 min and cooled, then the volume was reduced to 5 mL. The solution was stored overnight at 4°C. The deep red crystals that had formed were collected, washed with Et_2O, and dried in vacuo to afford the biladiene dihydrobromide salt **12** (186 mg, 0.28 mmol, 56%) as a metallic black-green crystalline solid.

Physical data: m.p. 206°C (dec); ^{1}H NMR (300 MHz, $CDCl_3$): δ = 9.81 (br s, 2H), 9.06 (br s, 2H), 7.75 (d, J = 3.4 Hz, 2H), 7.71 (d, J = 4.1 Hz, 1H), 7.65 (d, J = 3.7 Hz, 1H), 2.69 (q, J = 7.7 Hz, 4H), 2.47 (q, J = 7.7 Hz, 4H), 2.30 (s, 6H), 2.25 (s, 6H), 1.68 (s, 6H), 1.22–1.16 ppm (m, 12H); ^{13}C NMR (75.5 MHz, $CDCl_3$): δ = 159.35, 148.95, 145.77, 141.95, 131.81, 126.92, 126.76, 124.51, 122.35, 40.35, 28.01, 18.19, 17.87, 16.64, 14.20, 10.62, 9.85 ppm; IR (KBr): $\tilde{\nu}$ = 1607, 1423, 1263, 1157, 1119, 1040, 932, 804, 735, 678 cm^{-1}; UV/Vis (CH_2Cl_2): λ (ε) = sh 308 (5400), 350 (7500), sh 476 (31200), 519 nm (49100 mol^{-1}dm^{3}cm^{-1}); elemental analysis calcd (%) for $C_{33}H_{46}N_4Br_2$: C 60.19, H 7.04, N 8.51; found: C 59.94, H 6.80, N 8.30.

*7,8,10,10,12,13-Hexamethyl-2,3,17,18-tetraethylbiladiene-ac (free base, that is, **12**–2 HBr)*: A solution of the biladiene dihydrobromide **12** (60 mg, 91 μmol) in CH_2Cl_2 (30 ml) was washed with 2M NaOH (aq), H_2O, and then with 10% $Na_2S_2O_3$ (aq). The resulting yellow solution was dried over Na_2SO_4 and filtered, and the solvents were removed in vacuo. The crude product was dissolved in CH_2Cl_2 and filtered through Al_2O_3. Subsequent recrystallization from CH_2Cl_2/MeOH afforded orange needles that were washed with MeOH and dried under vacuum (38 mg, 78 μmol, 85%).

Physical data: m.p. 210–211°C; ^{1}H NMR (300 MHz, $CDCl_3$): δ = 6.92 (s, 2H), 6.70 (s, 2H), 3.49 (s, 2H), 2.62 (q, J = 7.6 Hz, 4H), 2.48 (q, J = 7.6 Hz, 4H), 2.04 (s, 6H), 1.72 (s, 6H), 1.58 (s, 6H), 1.23–1.16 ppm (m, 12H); ^{13}C NMR (75.5 MHz, $CDCl_3$): δ = 174.18, 146.50, 140.11, 133.28, 130.23, 129.24, 126.88, 124.66, 115.80, 41.84, 25.81, 18.16, 17.60, 16.79, 14.96, 10.40, 9.57 ppm; IR (KBr): $\tilde{\nu}$ = 2360, 1613, 1427, 1404, 1274, 1249, 1200, 1027, 937, 787, 707 cm^{-1}; UV/Vis (CH_2Cl_2): λ (ε) = 225 (176000), sh 349 (7600), 455 nm (35600 mol^{-1}dm^{3}cm^{-1}); FAB$^+$ MS: m/z (%): calcd for $C_{33}H_{42}N_4$: 496.8; found: 497.3 (82); elemental analysis calcd (%) for $C_{33}H_{42}N_4$: C 80.11, H 8.56, N 11.33; found: C 79.86, H 8.72, N 11.13.

*2,3,17,18-Tetraethyl-7,8,10,10,12,13-hexamethylisocorrolato–nickel(II) (**7**)*: Nickel(II)acetate tetrahydrate (125 mg, 0.5 mmol) was added to a solution of **12** (110 mg, 167 μmol) in MeOH (80 mL). The deep orange-red solution was stirred for 15 min, then chloranil (60 mg, 244 μmol) was added. Within minutes the solution turned brownish-green and a fine solid began to precipitate. The mixture was stirred for one hour at ambient temperature, then stored at 4°C for 12 h. The precipitate was collected, washed with MeOH, and then recrystallized from $CHCl_3$/MeOH (1:3) to afford blue needles of **7** that were once more washed with MeOH and dried in vacuo (63 mg, 114 μmol, 68%).

Physical data: m.p. 287–288°C; ^{1}H NMR (300 MHz, $CDCl_3$): δ = 7.09 (s, 2H), 2.77–2.65 (m, 8H), 2.29 (s, 6H), 2.25 (s, 6H), 1.68 (s, 6H), 1.52 (s, 6H), 1.26–1.18 ppm (m, 12H). ^{13}C NMR (75.5 MHz, [D_8]toluene): δ = 165.23, 150.20, 141.62, 141.16, 135.24, 132.88, 129.81, 124.29, 117.49, 39.24, 19.27, 18.38, 17.93, 17.87, 17.75, 14.00, 10.28 ppm; IR (KBr): $\tilde{\nu}$ = 1610, 1273, 1202, 1103, 1017, 953, 877, 843, 795, 760 cm^{-1}; UV/Vis (CH_2Cl_2): λ (ε) = 230 (26500), 248 (27100), sh 290 (9100), 367 (15800), 404 (52800), 427 (47000), sh 510 (8300), 541 (11400), 577 (12400), sh 636 (3900), 712 (2100), 784 (4000), 862 nm (8300 mol^{-1}dm^{3}cm^{-1}); FAB$^+$ MS: m/z (%): calcd for $C_{33}H_{40}N_4Ni$: 551.4; found: 550.3 (100), 535.3 (14) [M–CH_3]$^+$; elemental analysis calcd (%) for $C_{33}H_{40}N_4Ni$: C 71.88, H 7.31, N 10.16; found: C 72.03, H 7.67, N 9.97.

Measurements: The absorption spectra of **5** and **7** were measured with a spectrophotometer Perkin–Elmer Lambda-19 in CH_2Cl_2 (Aldrich spectrograde) at room temperature.

The electrochemical measurements were carried out in a glove box (less than 3 ppm of H_2O and less than 2 ppm of O_2) at room temperature (25±2°C) in PhCN containing Bu_4NPF_6 (0.1M) in a classical three-electrode cell. The electrochemical cell was connected to a computerized multipurpose electrochemical device (PAR 273) interfaced with a PC computer. The working electrode was a platinum (Pt) disk electrode (diameter: 2 mm) used either motionless for cyclic voltammetry (V = 20 mV s^{-1} to 5 V s^{-1}) or as a rotating disk electrode. The auxiliary electrode and the pseudoreference electrode were platinum wires. All potentials are referenced to the ferrocenium/ferrocene (Fc^+/Fc) couple used as internal standard. Benzonitrile (PhCN, Aldrich, 99%) was dried before use for two days with $CaCl_2$ (anhydrous, Fluka, 97%) and distilled on P_2O_5 (Prolabo) under reduced pressure and inert atmosphere (argon). The main fraction was collected under argon and transferred into the glove box. The supporting electrolyte, Bu_4NPF_6 (Fluka, electrochemical grade) was dried in an oven (65°C) under vacuum for two days. Bu_4NPF_6 was dissolved in PhCN inside the glove box, and the solution was then percolated over activated alumina. The available potentials on the platinum working electrode ranged from −2.5 V/Fc to +1.8 V/Fc.

Calculations: All electronic-structure calculations were carried out on high-performance computers at the *Regionales Rechenzentrum Köln* with the Gaussian 98 suite of programs.[16] Geometries were optimized at the DFT level employing the B3LYP functional[17] and the split-valence basis set 6-31G*.[18] Excitation energies and oscillator strengths were determined by the INDO/S-CIS method with the γ-parametrization of Zerner et al (ZINDO).[19] The active space in these calculations comprised all occupied and virtual molecular orbitals.

 © 2003 Wiley-VCH Verlag GmbH & Co. KGaA, Weinheim

[1] a) E. Vogel, M. Bröring, J. Fink, D. Rosen, H. Schmickler, K. W. K. Chan, Y.-D. Wu, M. Nendel, D. A. Plattner, K. N. Houk, *Angew. Chem.* **1995**, *107*, 2705–2709; *Angew. Chem. Int. Ed. Engl.* **1995**, *34*, 2511–2515; b) M. Bröring, J. Jendrny, L. Zander, H. Schmickler, J. Lex, Y.-D. Wu, M. Nendel, J. Chen, D. A. Plattner, K. N. Houk, E. Vogel, *Angew. Chem.* **1995**, *107*, 2709–2711; *Angew. Chem. Int. Ed. Engl.* **1995**, *34*, 2515–2517.

[2] Isocorrole is analogous to the hypothetic porphyrin tautomer isoporphyrin (H. Scheer, J. J. Katz in *Porphyrins and Metalloporphyrins* (Ed.: K. M. Smith), Elsevier, Amsterdam, **1975**, p. 449). In one of our previous publications the name isocorrole was given to the corrole constitutional isomer corrole(2.0.1.0) (E. Vogel, B. Binsack, Y. Hellwig, C. Erben, A. Heger, J. Lex, Y.-D. Wu, *Angew. Chem.* **1997**, *109*, 2725–2728; *Angew. Chem. Int. Ed. Engl.* **1997**, *36*, 2612–2615). To avoid confusion it is suggested to denote corrole(2.0.1.0) by the trivial name corrolene. In light of this overlap, **1** might better be called spirodiisocorrole.

[3] E. Vogel, M. Michels, L. Zander, J. Lex, N. S. Tuzun, K. N. Houk, *Angew. Chem.* **2003**, *115*, 2964–2969; *Angew. Chem. Int. Ed.* **2003**, *42*, 2857–2862.

[4] H. E. Simmons, T. Fukunaga, *J. Am. Chem. Soc.* **1967**, *89*, 5208–5215.

[5] R. Hoffmann, A. Imamura, G. D. Zeiss, *J. Am. Chem. Soc.* **1967**, *89*, 5215–5220.

[6] For a review of spiroconjugation see: H. Dürr, R. Gleiter, *Angew. Chem.* **1978**, *90*, 591–601; *Angew. Chem. Int. Ed. Engl.* **1978**, *17*, 559–569.

[7] Several spiro compounds consisting of two different π-systems have also been investigated. In these cases however the evidence for the occurrence of spiroconjugation is much less clear-cut. See: R. Gleiter, H. Hoffmann, H. Irngartinger, M. Nixdorf, *Chem. Ber.* **1994**, *127*, 2215–2224; and references therein.

[8] a) C. Batich, E. Heilbronner, E. Rommel, M. F. Semmelhack, J. S. Foos, *J. Am. Chem. Soc.* **1974**, *96*, 7662–7668; b) R. Gleiter, J. Uschmann, *J. Org. Chem.* **1986**, *51*, 370–380; c) M. Kobayashi, R. Gleiter, D. L. Coffen, H. Bock, W. Schulz, U. Stein, *Tetrahedron* **1977**, *33*, 433–439; d) A. Schweig, U. Weidner, D. Hellwinkel, W. Krapp, *Angew. Chem.* **1973**, *85*, 360–361; *Angew. Chem. Int. Ed. Engl.* **1973**, *12*, 310–311; e) A. Schweig, U. Weidner, R. K. Hill, D. A. Cullison, *J. Am. Chem. Soc.* **1973**, *95*, 5426–5427; f) A. Schweig, U. Weidner, J. G. Berger, W. Grahn, *Tetrahedron Lett.* **1973**, *14*, 557–560; g) K. Banert, F. Köhler, K. Kowski, B. Meier, B. Müller, P. Rademacher, *Chem. Eur. J.* **2002**, *8*, 5089–5093.

[9] a) G. Hohlneicher, *Ber. Bunsen-Ges.* **1967**, *71*, 917; b) R. Boschi, A. S. Dreiding, E. Heilbronner, *J. Am. Chem. Soc.* **1970**, *92*, 123–128; c) M. F. Semmelhack, J. S. Foos, S. Katz, *J. Am. Chem. Soc.* **1973**, *95*, 7325–7336; d) S. Smolinski, M. Balazy, H. Iwamura, T. Sugawara, Y. Kawada, M. Iwamura, *Bull. Chem. Soc. Jpn.* **1982**, *55*, 1106–1111; e) J. Spanget-Larsen, J. Uschmann, R. Gleiter, *J. Phys. Chem.* **1990**, *94*, 2334–2344; f) B. H. Boo, Y. S. Choi, T.-S. Kim, S. K. Kang, Y. H. Kang, S. Y. Lee, *J. Mol. Struct.* **1996**, *377*, 129–136.

[10] a) T. Haumann, J. Benet-Buchholz, R. Boese, *J. Mol. Struct.* **1996**, *374*, 299–304; b) J. V. Raman, K. E. Nielsen, L. H. Randall, L. A. Burke, G. I. Dmitrienko, *Tetrahedron Lett.* **1994**, *35*, 5973–5976.

[11] A. W. Johnson, I. T. Kay, *J. Chem. Soc.* **1965**, 1620–1629.

[12] H. Xie, K. M. Smith, *Tetrahedron Lett.* **1992**, *33*, 1197–1200.

[13] Crystal data for **7**: $C_{33}H_{40}N_4Ni$, $M=551.40$, crystals from $CHCl_3$/MeOH, $0.20\times0.15\times0.15$ mm, monoclinic, $a=13.071(1)$, $b=16.403(1)$, $c=13.371(1)$ Å, $\beta=93.08(1)°$, $V=2862.6(5)$ Å^3, $T=293(2)$ K, space group $P2_1/c$, $Z=4$, $d_{calcd}=1.279$ g cm^{-3}, $\mu=0.706$ mm^{-1}, $2\Theta_{max}=54°$, $Mo_{K\alpha}$ radiation ($\lambda=0.71073$ Å), graphite monochromator, φ/ω scans. A total of 12215 reflections were measured, of which 6235 ($R_{int}=0.018$) were unique. Final residuals were $R1=0.0371$ and $\omega R2=0.094$ (for 4838 observed reflections with $I>2\sigma(I)$, 504 parameters) with GOF 1.017 and largest residual peak 0.22 e Å^{-3} and hole -0.19 e Å^{-3}. All data were collected on a Nonius KappaCCD diffractometer. The structure was solved by using direct methods (SHELXS-97, G. M. Sheldrick, *Program for the Solution of Crystal Structures*, University of Göttingen, Germany, **1997**), and refined against F^2 for all independent reflections (heavy atoms with anisotropic temperature factors, H atoms with isotropic parameters, SHELXL-97, G. M. Sheldrick, *Program for the Refinement of Crystal Structures*, University of Göttingen, Germany, **1997**).
CCDC-209299 contains the supplementary crystallographic data for this paper. These data can be obtained free of charge via www.ccdc.cam.ac.uk/conts/retrieving.html (or from the Cambridge Crystallographic Data Centre, 12 Union Road, Cambridge CB2 1EZ, UK; fax: (+44) 1223-336-033; or deposit@ccdc.cam.uk).

[14] The calculated oscillator strengths of all transitions are substantially larger than the experimental values, but such an overestimation is not uncommon for the INDO/S method (ref. [19a]).

[15] a) A. S. Davydov, *The Theory of Molecular Excitons*, McGraw–Hill, New York, **1962**; b) M. Kasha, H. R. Rawls, M. A. El-Bayoumi, *Pure Appl. Chem.* **1965**, *11*, 371–392.

[16] Gaussian 98 (Revision A.7), M. J. Frisch, G. W. Trucks, H. B. Schlegel, G. E. Scuseria, M. A. Robb, J. R. Cheeseman, V. G. Zakrzewski, J. A. Montgomery, R. E. Stratmann, J. C. Burant, S. Dapprich, J. M. Millam, A. D. Daniels, K. N. Kudin, M. C. Strain, O. Farkas, J. Tomasi, V. Barone, M. Cossi, R. Cammi, B. Mennucci, C. Pomelli, C. Adamo, S. Clifford, J. Ochterski, G. A. Petersson, P. Y. Ayala, Q. Cui, K. Morokuma, D. K. Malick, A. D. Rabuck, K. Raghavachari, J. B. Foresman, J. Cioslowski, J. V. Ortiz, B. B. Stefanov, G. Liu, A. Liashenko, P. Piskorz, I. Komaromi, R. Gomperts, R. L. Martin, D. J. Fox, T. Keith, M. A. Al-Laham, C. Y. Peng, A. Nanayakkara, C. Gonzalez, M. Challacombe, P. M. W. Gill, B. G. Johnson, W. Chen, M. W. Wong, J. L. Andres, M. Head-Gordon, E. S. Replogle, J. A. Pople, Gaussian, Inc., Pittsburgh, PA, **1998**.

[17] a) A. D. Becke, *J. Chem. Phys.* **1992**, *96*, 2155–2160; b) A. D. Becke, *J. Chem. Phys.* **1993**, *98*, 5648–5652; c) C. Lee, W. Yang, R. G. Parr, *Phys. Rev. B* **1988**, *37*, 785–789.

[18] P. C. Hariharan, J. A. Pople, *Theor. Chim. Acta* **1973**, *28*, 213–222.

[19] a) J. Ridley, M. Zerner, *Theor. Chim. Acta* **1973**, *32*, 111–134; b) A. D. Bacon, M. C. Zerner, *Theor. Chim. Acta* **1979**, *53*, 21–54; c) M. C. Zerner, G. H. Loew, R. F. Kirchner, U. T. Mueller-Westerhoff, *J. Am. Chem. Soc.* **1980**, *102*, 589–599.

Received: May 2, 2003 [F5094]

© 2003 Wiley-VCH Verlag GmbH & Co. KGaA, Weinheim